

Image Analysis Method for Quantifying Snow Losses on PV Systems

Snow Accumulation on PV Modules

With the precipitous drop in the cost of installed solar, both centralized and distributed PV systems are seeing exponential growth in northern latitudes. As a result, investors and asset owners are increasingly concerned about the impact of snow and ice on system lifetime rates-of-return. The Snow as a Factor of PV Performance and Reliability project aims to address the physical and meteorological contributors to snow shedding as well as the overall performance and reliability of northern PV systems. Here we present a new method for quantifying, and analyzing snow shedding rates and related energy losses.



Snow accumulation and persistence concerns for photovoltaic arrays include:

- Immediate decrease or cease of power generation due to shading
- Physical damage to glass, frame, or racking
- Accelerated degradation of inner components via
 - Mechanical stress on module due to heavy accumulation
 - Moisture ingress
 - Freeze/thaw cycling

Therefore our research more broadly aims to:

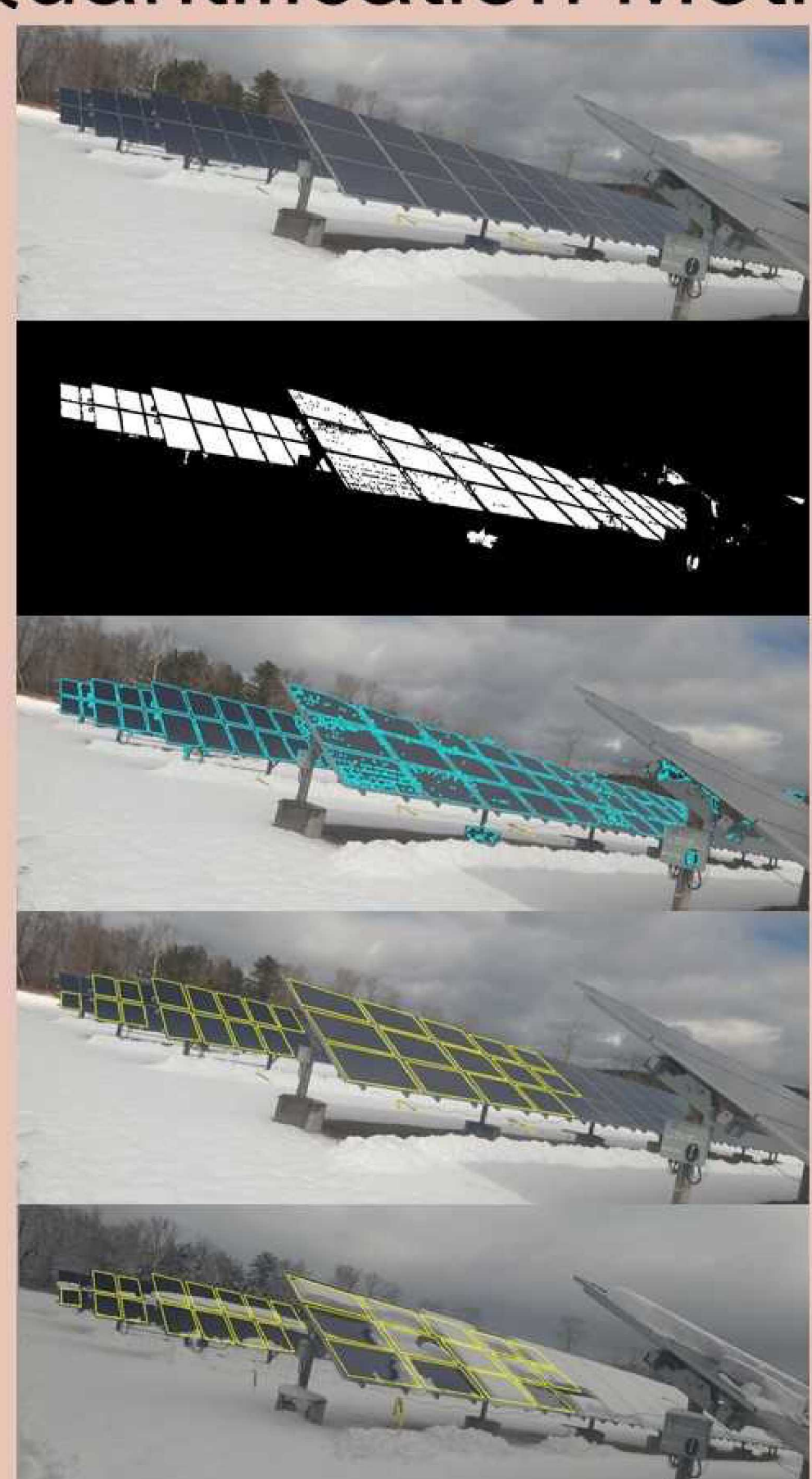
1. Identify mitigation strategies to reduce snow losses
2. Develop system-level design recommendations for PV installations that regularly see snow.

Snow Shedding Quantification Method

Step 1: Extract Module Time-Series Images

1. Stabilize full-field images via image registration to compensate for camera movement.
2. Select a snow-free field image.
3. Segment the snow-free image by cell color in hue-saturation-value color space.
4. Determine module boundaries via contour algorithm.
5. Approximate contours as quadrilaterals.
6. Filter quadrilaterals by area.
7. Planar-index quadrilateral regions of each field image into images proportional to the actual module dimensions.

This produces a time-series of images for each module.



Step 2: Map Module Snow Coverage

Segment each module-level image by snow and non-snow color in hue/saturation/value color space. A time-series of binarized module-level images (example below) is assembled into a GIF for visualization.



The distribution of snow coverage is considered for power modeling in Step 3.

Step 3: Model Power Output

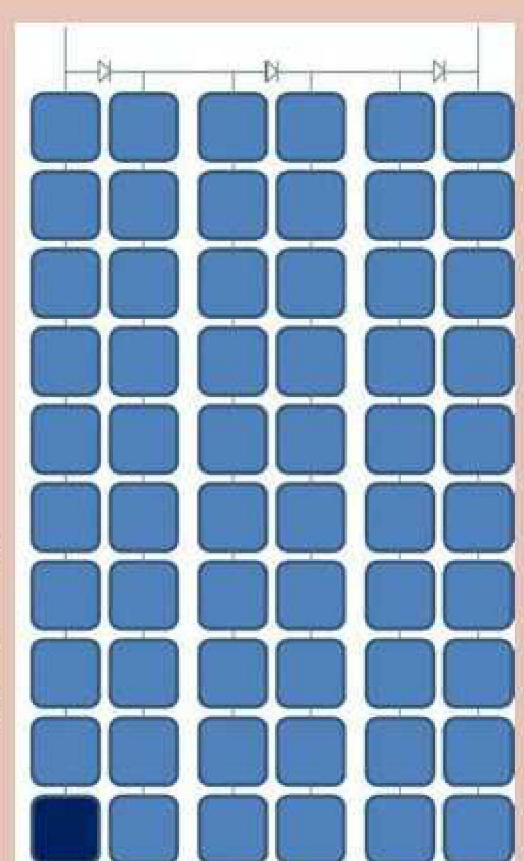
The % I_{sc} of a string is equal to the complement of the highest % coverage for any cell in that string. In a module-level I-V curve, strings are added in voltage in order of decreasing I_{sc} . So each local maximum power point is calculated:

$$\%P_n = \frac{n}{3} \times \%I_{sc,n}$$

$$= \frac{n}{3} \times (100 - \%coverage_{max-n})$$

where $n=1$ for the highest I_{sc} string, $n=3$ for the lowest

Module power is the largest of these local maxima.

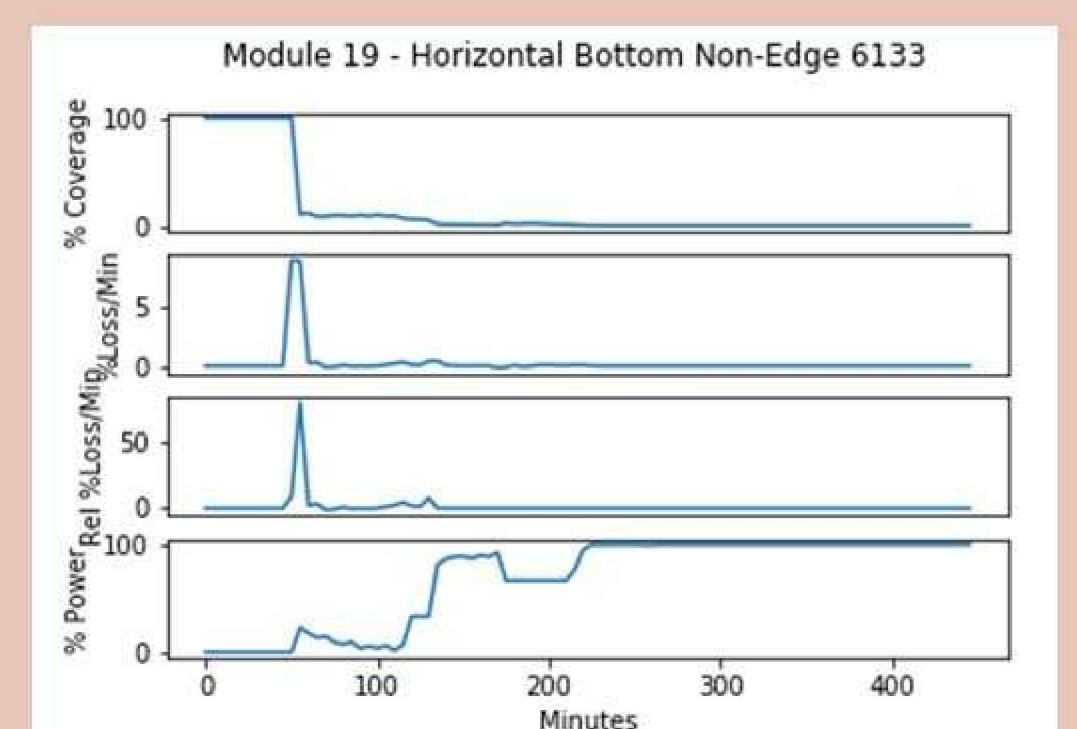


Step 4: Quantify Shedding Rates

From the time-series of percent coverage and percent, we can generate metrics for instantaneous shedding rate (% coverage shed per minute), and several other metrics:

- Total energy yield
- Shedding start time
- Power production start time
- 90% power production time
- Shedding finish time (full power)

The relative differences in these times are useful for comparing the shedding behavior of different modules and arrays.

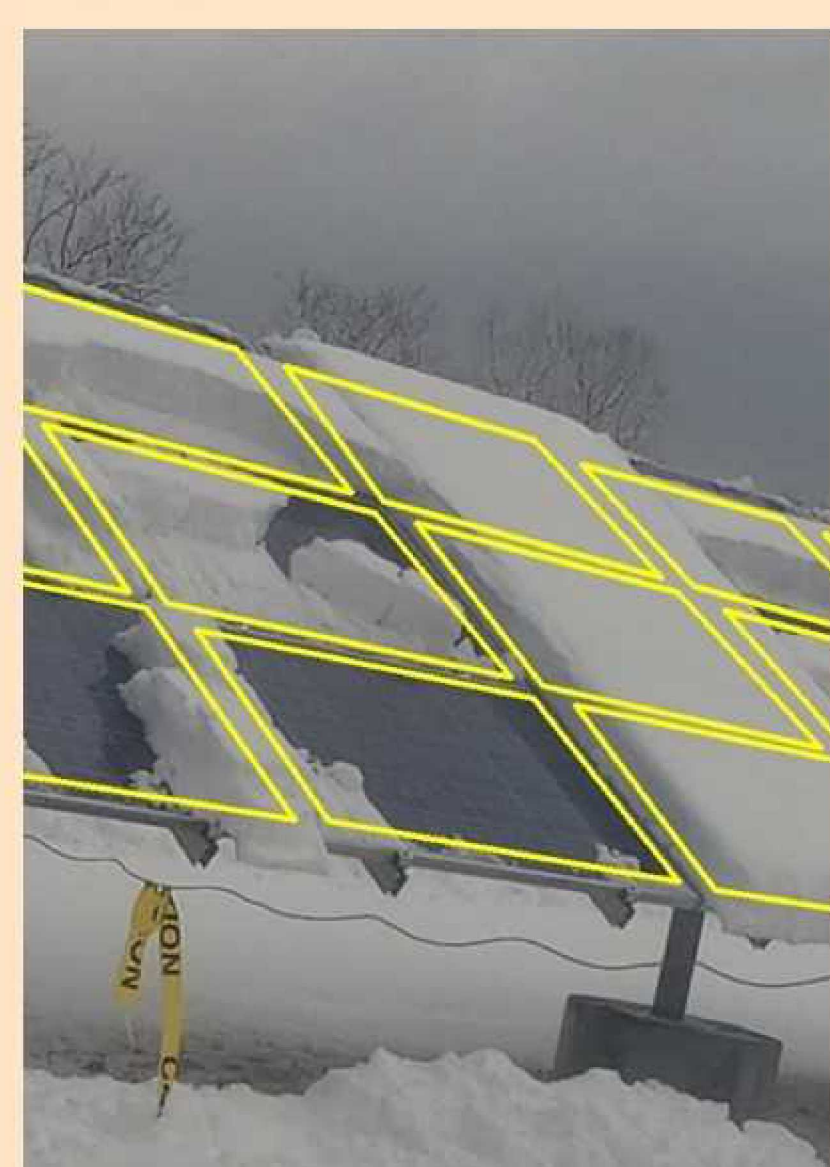


Snow Quantification Errors

Camera angle affects perceived snow coverage. Low camera angles lead to:

- Overestimation of snow coverage by snow coverage on adjacent modules
- Misclassification of vertical snow faces as clear module area (by color)

Additionally, heavy snowfall can cause deflection of modules or arrays that prevent accurate module area extraction. In this case, the lightly colored module frame is included in the extracted image and is classified as snow, inaccurately decreasing the modeled power. These errors can be decreased by camera placement normal to the module face.



Module Orientation Case Study

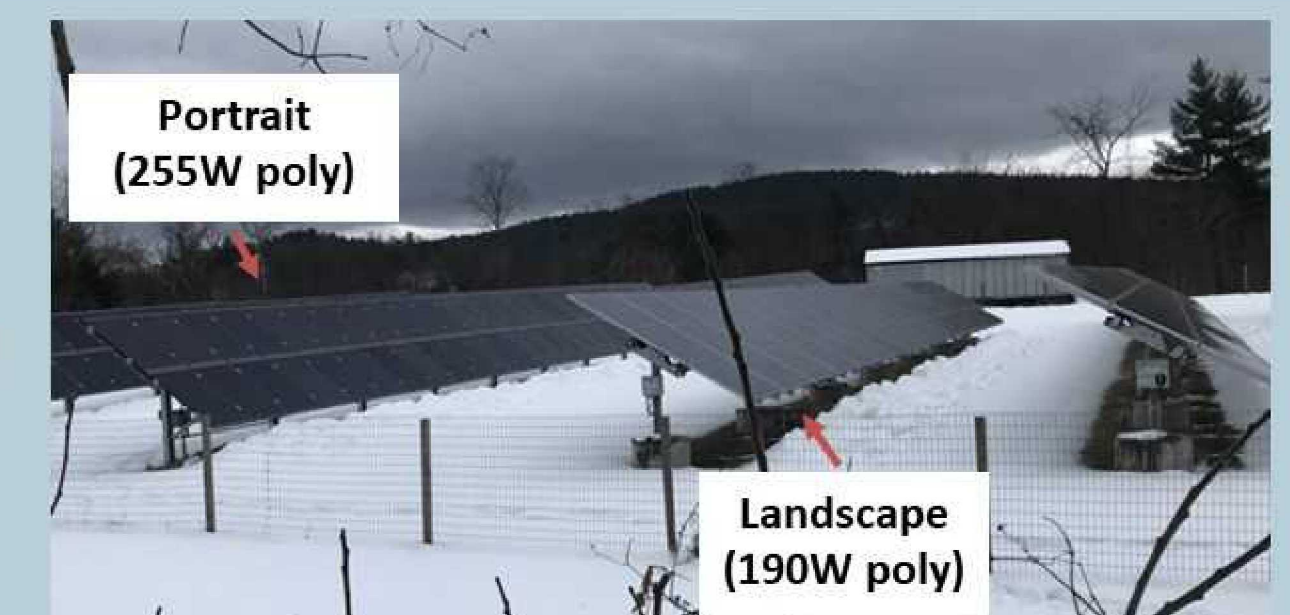
A 132kW PV site in Vermont with two adjacent ground mount, 30° fixed tilt PV systems:

- 58kW array (190W 60 cell poly c-Si modules) in landscape orientation
- 74kW system (255W 60 cell poly c-Si modules) portrait orientation

A monitoring system collects irradiance and backsheet temperature data, and digital images at 5-minute intervals.

One 9" snowfall event was captured on March 24th, 2020, and subsequent snow shedding of both arrays was captured on March 25th. There was no appreciable difference in temperature data for the two arrays during this time.

Time-series images were extracted and analyzed for 28 modules: 14 portrait and 14 landscape as shown above left.

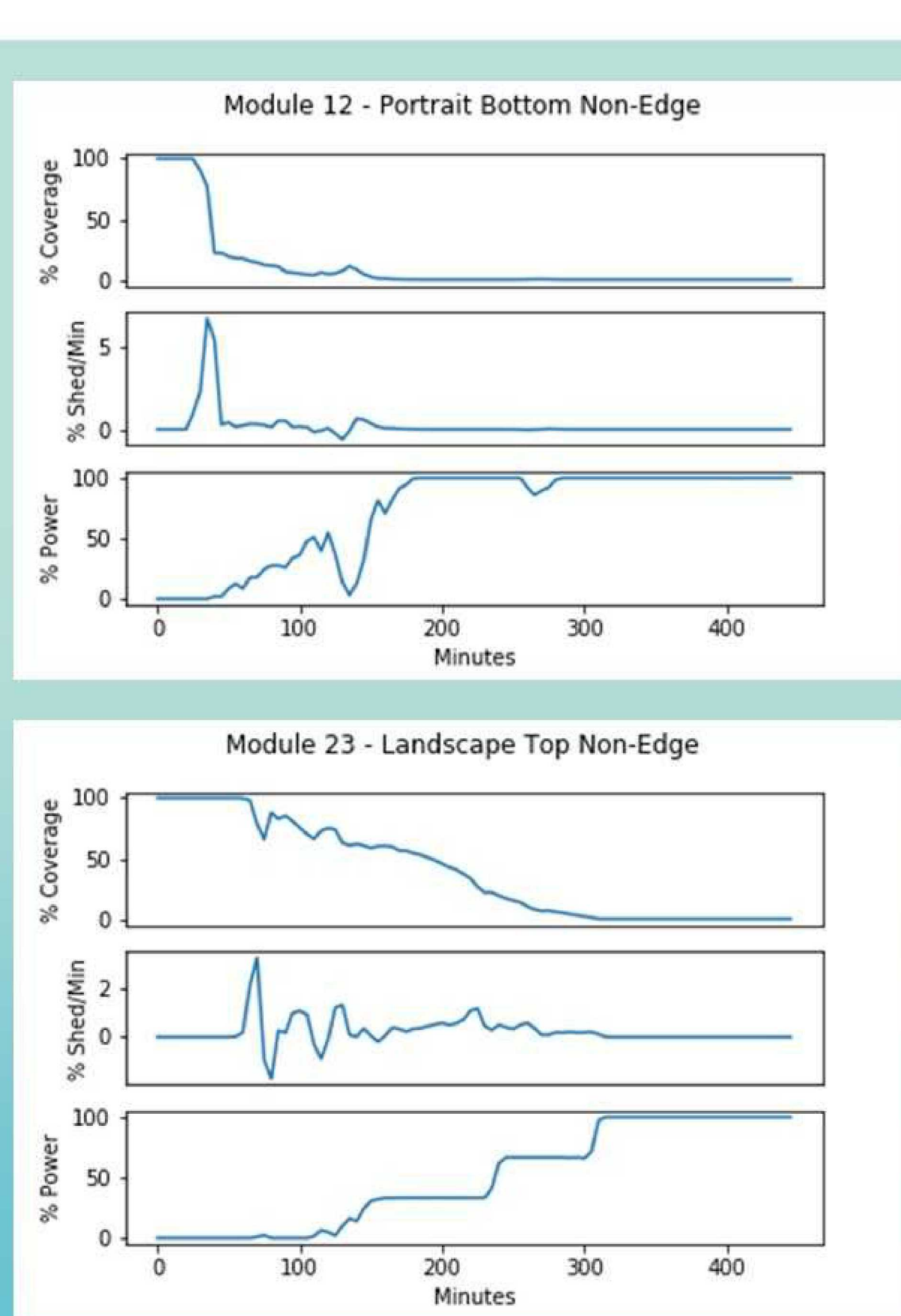


Data	Make/Model	Data description
Digital images	Go-Pro Hero8	Images collected and stored at an interval of 5 minutes during daylight hours
Back-of-module temperature	Omega, Type T	One sensors affixed to each of two designated mid-row modules for each module type
Datalogger	Campbell CR-1000	Data collected at a frequency of 15 secs; averaged per minute

Case Study Results

Median results for each module type by orientation, position and proximity to the edge of the array are given below. Portrait modules generally outperformed landscape in energy yield and shedding time. Module position also plays a large role in shedding behavior, with modules at the edge and bottom of the array shedding and producing power earlier than top row or non-edge modules.

Orientation	Position	Edge	Energy yield (%)	Time to start shed (min)	Time to produce power (min)	Time to 90% power (min)	Time to finish shed (min)
Portrait	Top	Edge	80.2	25	72.5	97.5	125
Portrait	Bottom	Edge	74.7	25	35	230	240
Portrait	Top	Non-Edge	64.7	30	115	185	225
Portrait	Bottom	Non-Edge	72.8	30	37.5	182.5	230
Landscape	Top	Edge	54.8	45	70	275	280
Landscape	Middle	Edge	60.5	45	45	285	285
Landscape	Bottom	Edge	66.0	45	55	285	290
Landscape	Top	Non-Edge	55.0	57.5	72.5	310	310
Landscape	Middle	Non-Edge	54.1	37.5	65	357.5	357.5
Landscape	Bottom	Non-Edge	68.1	55	65	330	335



References

1. R. E. Pawluk et al., "Photovoltaic electricity generation loss due to snow—a literature review on influence factors, estimation, and mitigation," *Renewable and Sustainable Energy Reviews*, vol. 107, pp. 171–182, 2019.
2. R. W. Andrews et al., "The effects of snowfall on solar photovoltaic performance," *Solar Energy*, vol. 92, pp. 84–97, 2013.
3. E. Andenæs et al., "The influence of snow and ice coverage on the energy generation from photovoltaic solar cells," *Solar Energy*, vol. 159, pp. 318–328, 2018.
4. C. Good et al., "Solar cells above the arctic circle—measuring characteristics of solar panels under real operating conditions," in *24th EU-PVSEC*, 2009, pp. 21–25.
5. T. Townsend and L. Powers, "Photovoltaics and snow: An update from two winters of measurements in the sierra," in *37th IEEE PVSC*, 2011, pp. 003 231–003 236.
6. B. Marion et al., "Measured and modeled photovoltaic system energy losses from snow for Colorado and Wisconsin locations," *Solar Energy*, vol. 97, pp. 112–121, 2013.
7. "The impact of snow on pv performance." [Online]. Available: <https://energy.sandia.gov/programs/renewable-energy/solar-energy/photovoltaics/pv-systems-and-reliability/snow-as-a-factor-in-photovoltaic-performance-and-reliability/>
8. A. M. Karimi et al., "Automated pipeline for photovoltaic module electroluminescence image processing and degradation feature classification," *IEEE Journal of Photovoltaics*, vol. 9, no. 5, pp. 1324–1335, 2019.
9. L. Burnham et al., "Performance of bifacial photovoltaic modules on a dual-axis tracker in a high-latitude, high-albedo environment," in *IEEE 46th PVSC*, 2019, pp. 1320–1327.
10. D. Riley et al., "Differences in snow shedding in photovoltaic systems with framed and frameless modules," in *IEEE 46th PVSC*, 2019, pp. 0558–0561.
11. J. Bogenrieder et al., "Technology-dependent analysis of the snow melting and sliding behavior on photovoltaic modules," *Journal of Renewable and Sustainable Energy*, vol. 10, no. 2, p. 021005, 2018.
12. A. Granlund et al., "The influence of module tilt on snow shadowing of frameless bifacial modules," in *36th EU-PVSEC*, 2019, pp. 1646–1650.